Theory of optical transmission through elliptical nanohole arrays

Yakov M. Strelniker*

Minerva Center, Jack and Pearl Resnick Institute of Advanced Technology, and Department of Physics, Bar-Ilan University, IL–52900 Ramat-Gan, Israel

(Received 1 February 2007; revised manuscript received 29 April 2007; published 8 August 2007)

We present a theory that explains (in the quasistatic limit) the experimentally observed [R. Gordon *et al.*, Phys. Rev. Lett. **92**, 037401 (2004)] squared dependence of the ratio of polarizations on the aspect ratio of the holes, as well as other features of extraordinary light transition. We calculated the effective dielectric tensor of a metal film penetrated by elliptical cylindrical holes and found the extraordinarily light transmission at special frequencies related to the surface plasmon resonances of the composite film. We also propose to use the magnetic field for getting a strong polarization effect, which depends on the ratio of the cyclotron to plasmon frequencies.

DOI: 10.1103/PhysRevB.76.085409 PACS number(s): 78.67.−n, 78.66.Sq

I. INTRODUCTION

A pioneering paper of Ebbesen *et al.*[1] reported on an extraordinary optical transmission through periodic holes array in metallic films. This was explained by the coupling of light with surface plasmons, the latter being treated as coupled waves, propagating along both film surfaces (in framework of the theory described in Ref. 2). Since Ref. 1 the study of the transmission properties of subwavelength apertures has become a very active area of research in electromagnetism,[3] which stimulates the development of many new analytical and numerical approaches. Even though many of these methods were based on a Fourier expansion of hole arrays and as a consequence could take into account the hole shape through its Fourier transform,[4] most of the studies were restricted to the circular or square shapes of the holes. Only quite recently the nonisotropic shape of inclusions and their dramatic influence on the optical properties were taken into intensive studies. A system with *elliptical holes* was considered in the experimental work of Gordon *et al.* (see Ref. 5), and a system with *rectangular holes* was considered in the theoretical work of Sarrazin and Vigneron (see Ref. 6). Simultaneously with this, several other experimental[7–9] as well as theoretical[10,11] works have focused on the influence of the elliptical and rectangular hole shape on the optical transmission properties (of periodical arrays as well as single subwavelength holes). These papers have considered the polarization properties of the systems with nonisotropic holes and have stimulated big interest in this problem.[12–16] In particular, the polarization and huge enhancement properties of a single rectangular hole were studied theoretically in detail in Ref. 13.

We would like to note in this context, that in order to see the above-mentioned effects it is not necessary to have holes that are actually nonisotropic. Already in Ref. 17 (in which we have considered the effect of the applied static magnetic field on the extraordinary light transmission) we have shown that the presence of the magnetic field transforms the initially *circular* holes into effective holes that have an *elliptic* shape. This happens in the rescaled *virtual* coordinate space and through this introduces some *optical anisotropy* into the system. This was a particular case of a more general theory developed in Ref. 18, in which it was shown that the magneto-optical properties, as well as plasmon frequencies of the periodic metal-dielectric composite, depend upon the microstructure and can therefore be controlled by both the magnitude and the direction of the applied dc magnetic field.

In this paper we present a theory, which in the quasistatic (long wavelength) limit explains the squared dependence of the ratio of polarizations on the aspect ratio of the holes (experimentally observed in Ref. 5), as well as other optical features. This theory is a further development of our methods described in Refs. 17–20. We also note that similar effects (e.g., light polarization) can be reached by applying a static magnetic field. The possibility to affect the plasmons and the optical properties of nanosystems by applied magnetic field is also considered in Refs. 21 and 22.

The remainder of this paper is arranged as follows. In Sec. II, we describe our method of calculating the ratio of polarizations as well as the effective permittivity tensor $\hat{\varepsilon}_e$ for both random and ordered arrangements of elliptical holes in a metallic film. In Sec. III, we present numerical results for both cases, based on these expressions, followed by a brief discussion in Sec. IV.

II. FORMALISM

Let us consider a geometry which corresponds to the above-mentioned experiment:[5] a metal film with a square array of identical elliptical holes. A monochromatic light beam of angular frequency ω impinges upon this film along the perpendicular axis y, with linear polarization along the principal axis x of the array (see Fig. 1).

Following Refs. 17–20, we can treat the holes as dielectric inclusions embedded in a conducting host.[17,23] If the holes form a periodic lattice, as in experiments, this description is suitable, provided the lattice constant is much smaller than the wavelength, i.e., when the film is homogeneous on a scale of the electromagnetic wavelength. In this approach, the local electric potential $\phi^{(\alpha)}(\mathbf{r})$ is then the solution of a boundary value problem based upon the Laplace partial differential equation

$$\nabla \cdot \hat{\varepsilon}_M \cdot \nabla \phi^{(\alpha)} = \nabla \cdot \theta_I \delta\hat{\varepsilon} \cdot \nabla \phi^{(\alpha)}, \qquad (1)$$

and the boundary condition $\phi^{(\alpha)} = r_\alpha$. Here r_α is the α component of $\mathbf{r}$, $\hat{\varepsilon}_I$ and $\hat{\varepsilon}_M$ are the electrical permittivity tensors

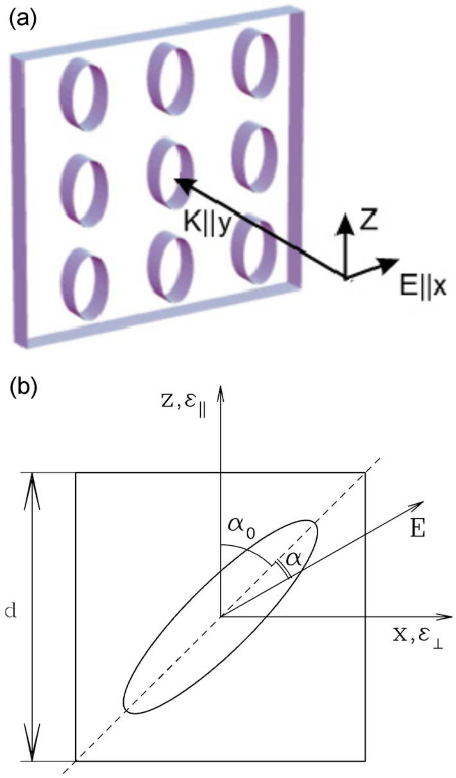

FIG. 1. (Color online) (a) A schematic drawing of a metal film with a periodic array of elliptical holes. The incident light beam is normal to the film surface, i.e., the *ac* electric field **E** is parallel to the film plane, while the wave vector is normal to it (i.e., $\mathbf{k}\parallel y$). (b) An elliptical hole in a unit cell when the main semiaxes a and c are inclined with respect to the lattice axes x and z by an angle α_0.

of the *inclusions* and the *metal* host, respectively, $\delta\hat{\varepsilon}\equiv\hat{\varepsilon}_M-\hat{\varepsilon}_I$, $\theta_I(\mathbf{r})$ is the characteristic function describing the location and the shape of the inclusions ($\theta_I=1$ inside the inclusions and $\theta_I=0$ outside of them).[17,23–25]

The host with the anisotropic permittivity tensor $\hat{\varepsilon}_M$ can be transformed to an isotropic $\hat{\varepsilon}'_M$ using the rescaling of the Cartesian coordinates ($\xi_1\equiv x/\sqrt{\varepsilon_{xx}}$, $\xi_2\equiv y/\sqrt{\varepsilon_{yy}}$, $\xi_3\equiv z/\sqrt{\varepsilon_{zz}}$). Then elliptic cylinder inclusion will be transformed into some new elliptic cylinder in the rescaled virtual ξ space, and the electric field $\mathbf{E}_I=\nabla\phi_I$ inside this single inclusion {inclined by some angle α_0 in respect to the main axes [see Fig. 1(b)]} can be found from the system of linear equations,[26,27]

$$E_\alpha^{(I)}=E_{0\alpha}+\sum_{\beta,\gamma}n_{\alpha\beta}\delta\varepsilon_{\beta\gamma}(\varepsilon_{\alpha\alpha}^{(M)}\varepsilon_{\beta\beta}^{(M)})^{-1/2}E_\gamma^{(I)}, \tag{2}$$

where $n_{\alpha\beta}$ are the Cartesian components of the depolarization factor.[26,27] The latter can be transformed to the diagonal form $n_{\alpha\beta}=n_\alpha\delta_{\alpha\beta}$ by a simple coordinate rotation $\mathbf{r}'=\hat{R}(\alpha_0)\cdot\mathbf{r}$, where α_0 is the angle on inclination of the elliptical holes from the lattice axes [see Fig. 1(b)], $\hat{R}(\alpha_0)$ is the rotation matrix

$$\hat{R}(\alpha_0)=\begin{pmatrix}\cos\alpha_0 & -\sin\alpha_0\\ \sin\alpha_0 & \cos\alpha_0\end{pmatrix}, \tag{3}$$

which directs the new coordinate axes along the principal ellipse axes. Note that $n_{\alpha\beta}$ (as well as n_α) now depends on the precise shape of the transformed inclusion, and therefore is a function of $\hat{\varepsilon}_M$. If the coordinate axes are the principal axes of the inclusion ($n_{\alpha\beta}=n_\alpha\delta_{\alpha\beta}$), then the elliptic cylindric hole of the semiaxes a and c (with symmetry axis along y) transforms in ξ space into a new elliptic cylinder with semiaxes $a'=a/\sqrt{\varepsilon_{xx}}$ and $c'=c/\sqrt{\varepsilon_{zz}}$ for which

$$n_x=\frac{c'}{a'+c'}=\frac{c\sqrt{\varepsilon_{xx}}}{c\sqrt{\varepsilon_{xx}}+a\sqrt{\varepsilon_{zz}}}, \tag{4}$$

$$n_y=0,\quad n_z=1-n_x, \tag{5}$$

For simplicity, we assume the host permittivity tensor has the form $\hat{\varepsilon}=\varepsilon_0\hat{I}+i\frac{4\pi}{\omega}\hat{\sigma}$, where the conductivity tensor $\hat{\sigma}$ is taken in the free-electron Drude approximation with $\mathbf{B}_0\parallel z$,

$$\hat{\sigma}=\frac{\omega_p^2\tau}{4\pi}\begin{pmatrix}\frac{1-i\omega\tau}{(1-i\omega\tau)^2+H^2} & \frac{-H}{(1-i\omega\tau)^2+H^2} & 0\\ \frac{H}{(1-i\omega\tau)^2+H^2} & \frac{1-i\omega\tau}{(1-i\omega\tau)^2+H^2} & 0\\ 0 & 0 & \frac{1}{1-i\omega\tau}\end{pmatrix}, \tag{6}$$

ε_0 is the scalar dielectric constant of the background ionic lattice, and $\hat{I}$ is the unit tensor. The magnetic field enters only through the Hall-to-Ohmic resistivity ratio $H\equiv\rho_H/\rho=\sigma_{xy}/\sigma_{xx}=\mu|\mathbf{B}_0|=\omega_c\tau$, where $\omega_c=eB/mc$ is the cyclotron frequency, τ is the conductivity relaxation time, $\omega_p=(4\pi e^2N_0/m)^{1/2}$ is the plasma frequency, N_0 is the charge carrier concentration, m is its effective mass, and μ is the Hall mobility.

When $\varepsilon_{xx}=\varepsilon_{zz}$ ($H=0$), we have $n_x=c/(a+c)$, $n_z=a/(a+c)$. However, when $H>0$ the depolarization factor has a complicated dependence on ω.

Solving the system of linear equations (2), we obtain the following expression for the uniform electric field inside the original elliptical cylinder (when $\mathbf{B}_0\parallel z$):

$$\mathbf{E}_I=\hat{\gamma}\cdot\mathbf{E}_0, \tag{7}$$

where $\hat{\gamma}$ is a 3×3 matrix whose nonzero components are $\gamma_{xx}=\varepsilon_{xx}/(\varepsilon_{xx}-n_x\delta\varepsilon_{xx})$, $\gamma_{xy}=n_x\delta\varepsilon_{xy}/(\varepsilon_{xx}-n_x\delta\varepsilon_{xx})$, $\gamma_{yy}=1$, $\gamma_{zz}=\varepsilon_{zz}/(\varepsilon_{zz}-n_z\delta\varepsilon_{zz})$.

A. Ratio of polarizations

From Eq. (7) it follows that the ratio of polarizations [i.e., the ratio of the light intensity I_x (polarized parallel to the x axis) to the light intensity I_z (polarized parallel to the z axis), and therefore proportional to $|E_x/E_z|^2$], can be written (in the case of $n_{\alpha\beta}=n_\alpha\delta_{\alpha\beta}$) as

$$\frac{I_x}{I_z}=\left|\sqrt{\frac{\varepsilon_{xx}^{(M)}}{\varepsilon_{zz}^{(M)}}}\left(\frac{c\sqrt{\varepsilon_{zz}^{(M)}\varepsilon_{xx}^{(M)}}+a\varepsilon_{zz}^{(I)}}{a\sqrt{\varepsilon_{zz}^{(M)}\varepsilon_{xx}^{(M)}}+c\varepsilon_{xx}^{(I)}}\right)\left(\frac{E_{0x}^{(I)}}{E_{0z}^{(I)}}\right)\right|^2. \tag{8}$$

Let us consider the case of zero magnetic field, $H=0$, when both the host and the inclusions are isotropic and, therefore,

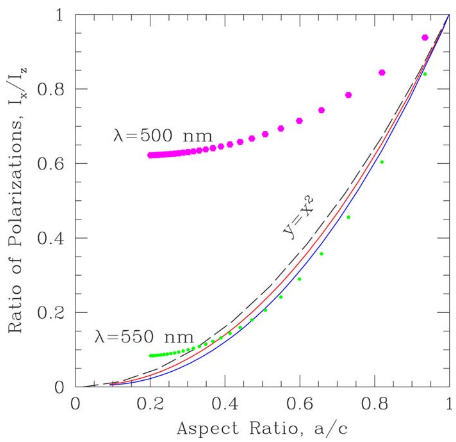

FIG. 2. (Color online) The ratio of polarizations of the transmitted light as a function of the aspect ratio a/c of the holes for different λ. For the values of λ from ~900 nm to ~700 nm the curves are close enough to the square law $y=x^2$ (left-hand dashed curve), while already for λ=550 nm and λ=500 nm (shown by dotted lines) the polarization ratio is essentially different from this law.

are characterized by the scalar tensors $\hat{\varepsilon}_M=\varepsilon_M\hat{I}$, $\hat{\varepsilon}_I=\varepsilon_I\hat{I}$ (where $\hat{I}$ is a unit matrix). We assume also that $E_{0x}=E_{0z}$. When $c\varepsilon_M \gg a\varepsilon_I$ and $a\varepsilon_M \gg c\varepsilon_I$, what might be true in the simple limit $\varepsilon_0 \ll \sigma/\omega$ and $\omega\tau \gg 1$ with $H=0$ (situation of Ref. 5), then from Eq. (8) it follows that

$$I_x/I_z = |E_x^{(I)}/E_z^{(I)}|^2 \simeq (c/a)^2, \tag{9}$$

as in Fig. 4 of Ref. 5.

In Fig. 2 we show the ratio (8) for different wavelengths, λ. Using the data[29] of the complex permittivity ε_M of the evaporated gold, we can see that in the wavelength's range between $\lambda\sim 900$ nm ($\varepsilon_M\sim -28.4+i1.8$) and $\lambda\sim 700$ nm ($\varepsilon_M\sim -14.7+i1.0$), the curves are close enough to the law $(c/a)^2$, while already for λ=500 nm (for which $\varepsilon_M\sim -2.7+i3.1$), the polarization ratio $|E_x/E_z|^2$ (shown by the dotted line) is essentially different from this law.

If $H\neq 0$ and $a=c$, then $I_x/I_z=|\varepsilon_{xx}/\varepsilon_{yy}|$ [see Eq. (8)]. In the Drude approximation (6) (and in the limit $\varepsilon_0\to 0$, $\omega_p\tau\to 1$) this takes the simplest form

$$I_x/I_z = |E_x/E_z|^2 = [1-(\omega_c/\omega)^2]^{-1}, \tag{10}$$

from which it follows that the ratio of polarizations I_x/I_z can be made arbitrarily large, since the value $\omega_c/\omega=(\omega_c/\omega_p)\times(\omega/\omega_p)^{-1}=(H/\omega_p\tau)(\omega/\omega_p)^{-1}$ [where $H\equiv\omega_c\tau$, see comments to Eq. (6)], can be made as close to 1 as necessary.

B. Effective permittivity tensor and surface plasmon resonances

Next, we approximately compute the tensor $\hat{\varepsilon}_e(\omega)$, which is defined by the relation $\hat{\varepsilon}_e\cdot\langle\mathbf{E}(\mathbf{r})\rangle=\langle\hat{\varepsilon}(\mathbf{r})\cdot\mathbf{E}(\mathbf{r})\rangle$, where $\langle\cdots\rangle$ denotes a volume average, and $\hat{\varepsilon}(\mathbf{r})$ is the local dielectric tensor. In the case of the dilute collection of the elliptic cylinders, the tensor $\hat{\varepsilon}_e$ takes the form[17,23–25] $\hat{\varepsilon}_e=\hat{\varepsilon}_M-p\,\delta\hat{\varepsilon}\cdot\hat{\gamma}$, where p is the volume fraction of inclusions. For the case $H=0$ (and when $\mathbf{E_0}$ and the coordinate axes are directed along the symmetry axes of the ellipse), $\hat{\varepsilon}_e$ takes the form

$$\varepsilon_{ii}^{(e)} = \varepsilon_M[1-p\,\delta\varepsilon_{ii}/(\varepsilon_M-n_i\delta\varepsilon_{ii})], \tag{11}$$

where n_i is given by Eq. (5), and $i=x,y,z$.

The frequency $\omega_{sp,i}$ of the surface plasmon (SP) polarized in the ith direction is the one in which $\mathbf{E}$ [see Eq. (7) and Eq. (11)] becomes very large even for a very small applied field. This condition is satisfied when $\varepsilon_{M;ii}(\omega_{sp,i})-n_i\delta\varepsilon_{ii}(\omega_{sp,i})=0$. Substituting Eq. (6) into this, and letting $\omega_p\tau\to\infty$, one obtains

$$\omega_{sp,i} = \omega_p\sqrt{(1-n_i)/[(1-n_i)+n_i\varepsilon_i^{(I)}]}. \tag{12}$$

For $\varepsilon_I=1$ this simplifies into $\omega_{sp,x}=\omega_p\sqrt{1-n_x}$.

In Maxwell-Garnett (MG) or Clausius-Mossotti approximation,[24,25] expressions for ε_e and ω_{sp} can be obtained directly from Eqs. (11) and (12), obtained in dilute approximation just by formal substitution $n_i\to n_i(1-p)$.[20]

When the aspect ratio c/a tends to infinity the considered geometry transforms into the case of the parallel slabs, which can be solved *exactly*, $1/\varepsilon_e=p_M/\varepsilon_M+p_I/\varepsilon_I$. Using the form (6), we can find the resonance frequency

$$\omega_{sp} = \omega_p\sqrt{p_I/(p_M\varepsilon_I+p_I)}. \tag{13}$$

This coincides with Eq. (12) in the limit $n_x\to 1$. The other exact solvable geometry, *parallel cylinders*, for which $n_i\to 0$, does not give any resonance, $\varepsilon_e=p_M\varepsilon_M+p_I\varepsilon_I=1-p_M(\omega_p/\omega)^2$.

C. Transmission coefficient

The dependence of the transmission coefficient T on frequency ω [as well as on the wavelength λ (see Fig. 4)] for different film thicknesses, can be obtained from the effective value ε_e using the known expression[20,28,30] for $T=|t|^2$, where

$$t = \frac{1-r_{12}^2}{\exp(-i\chi)-r_{12}^2\exp(i\chi)}, \tag{14}$$

and $r_{12}=(1-N)/(1+N)$, $N=\sqrt{\varepsilon_e(\omega)}$, $\chi=(\omega/c)hN=(\omega/\omega_p)\times(\omega_p h/c)N$, and h is the film thickness.[20,28,30]

D. Malus' law

Since the angular dependence of the permittivity tensor in the rotated coordinate system

$$\hat{\varepsilon}' = \hat{R}(\alpha+\alpha_0)\cdot\hat{\varepsilon}\cdot\hat{R}^{-1}(\alpha+\alpha_0) \tag{15}$$

[where $R(\alpha+\alpha_0)$ is given by Eq. (3) and α is the polarization angle, i.e., the angle between the vector $\mathbf{E}_0$ and the axes of the ellipse, see Fig. 1(b)] is a cosinelike

$$(\varepsilon_{xx}^{(e)})' = \varepsilon_{xx}^{(e)}\cos^2(\alpha+\alpha_0)+\varepsilon_{zz}^{(e)}\sin^2(\alpha+\alpha_0), \tag{16}$$

the angular dependence of the transmission coefficient $T(\alpha)$ appears (depending on the values of a/c and $\omega h/c$) also to be cosinelike. This explains the Malus' law[6,31] of the light transmission, T, observed in Refs. 5 and 31.

III. NUMERICAL RESULTS

When the holes are arranged on a two-dimensional periodic lattice[1,5] a more suitable approach is a Fourier expansion technique.[23] Since $\theta_I(\mathbf{r})$ and $\psi^{(\alpha)}=\phi^{(\alpha)}-r^{(\alpha)}$ are now periodical functions, they can be expanded in a Fourier series. This transforms Eq. (1) into an infinite set of linear algebraic equations for the Fourier coefficients

$$\psi_{\mathbf{g}}^{(\alpha)}=\frac{1}{V}\int_V \psi^{(\alpha)}(\mathbf{r})e^{-i\mathbf{g}\cdot\mathbf{r}}dV, \tag{17}$$

where $\mathbf{g}=(2\pi/d)(m_x,m_y,m_z)$ is a vector of the appropriate reciprocal lattice, m_i are the arbitrary integers, d is a lattice constant, and V is the volume of a unit cell. After solving a truncated, finite subset of those equations (in our calculations the range of arbitrary integers m_i is from -40 up to $+40$, in each direction[20]), we can use those Fourier coefficients $\psi_{\mathbf{g}}^{(\alpha)}$ in order to calculate the bulk effective macroscopic electric permittivity tensor $\hat{\varepsilon}_e$, using the procedure described in Refs. 17 and 23–25.

A. Elliptical holes

The Fourier coefficient $\theta_{\mathbf{g}}$ of the $\theta_I(\mathbf{r})$ function of the elliptical hole (inclined by the angle α_0 in respect to the main lattice axes) has the form[17,23]

$$\theta_{\mathbf{g}}=\frac{1}{V}\int_V \theta(\mathbf{r})e^{-i\mathbf{g}}dV=\frac{4\pi ac}{d^3\tilde{g}_\perp}J_1(\tilde{g}_\perp)\frac{\sin(|g_z|h/2)}{|g_z|}, \tag{18}$$

where $J_1(x)$ is a Bessel function and $\tilde{g}_\perp(\alpha)=[a^2(g_x\cos\alpha+g_z\sin\alpha)^2+c^2(g_z\cos\alpha-g_x\sin\alpha)^2]^{1/2}$.

In Figs. 3(a) and 3(b) we show the imaginary and real parts of $\varepsilon_e(\omega)$ vs ω/ω_p, respectively. The curves without points are the two principal in-plain components $\varepsilon_{xx}^{(e)}$ and $\varepsilon_{zz}^{(e)}$ (corresponding to polarizations $\mathbf{E_0}\|x$ and $\mathbf{E_0}\|z$, respectively) as obtained in the dilute and MG approximation. The full and open squares in Fig. 3(a) denote the same quantities, but now for a square lattice (of lattice constant d) of elliptical holes with the same aspect ratio and volume (surface in two dimensions) fraction p as in MG and dilute approximations. In this case, $\varepsilon_{xx}^{(e)}$ and $\varepsilon_{zz}^{(e)}$ are calculated by the Fourier expansion technique[17] mentioned above.

Finally, in Fig. 3(c), we show the calculated [using Eq. (14)] transmission coefficient $T(\omega)$ for the dielectric functions shown in Figs. 3(a) and 3(b). This coefficient shows the characteristic "extraordinary transmission." Both approximations show rather sharp SP peaks in the transmission, which occur at different frequencies depending on the polarization of the incident radiation. They occur at slightly different frequencies from the SP peaks themselves. This is the expected behavior, since the SP peaks correspond to *absorption* maxima. In fact, the transmission peaks occur at frequencies which correspond closely to the maxima in the *real part* of $\varepsilon_e(\omega)$ for the chosen polarization.

The amplitudes and frequencies of the peaks (for both polarizations $\mathbf{E_0}\|x$ and $\mathbf{E_0}\|z$) depend on the aspect-ration a/c. For polarization along the z axis the resonance frequency ω_{spz} shifts for a larger value and its amplitude reduces drastically. Estimating the imaginary part of $\delta\varepsilon_{ii}^{(e)}\equiv\varepsilon_{ii}^{(e)}-\varepsilon_M$ [see Eq. (11)] at the resonance frequency ω_{spi}, we found that the ratio $\mathrm{Im}\,\delta\varepsilon_{xx}^{(e)}(\omega_{spx})/\mathrm{Im}\,\delta\varepsilon_{zz}^{(e)}(\omega_{spz})$ is of the order $\sim(n_x/n_z)^{5/2}=(c/a)^{5/2}$. For the aspect ratio $a/c=0.3$ this is of the order ~ 20, in agreement with our numerical calculations [see Fig. 3(a)]. One might expect that in the extraordinary light transition the maximum at ω_{spz} will also be much smaller when compared to the maximum at ω_{spx}, but [as we can see in Figs. 3(c) and 4] they are of the same order. In Fig. 4 we show the data, presented in Fig. 3(c), in terms of wavelength λ. The calculations were performed for the systems with aspect ratio $a/c=0.33$, surface fraction of holes, $p=0.094$, $\varepsilon_I=1$, $\xi=\omega_p h/c=1$, $\omega_p\tau=40$, $\omega_p=3\times10^{15}$ rad/s (typical for the Au value,[5] so that $\omega_p h/c=1$), and the film thickness $h=100$ nm.

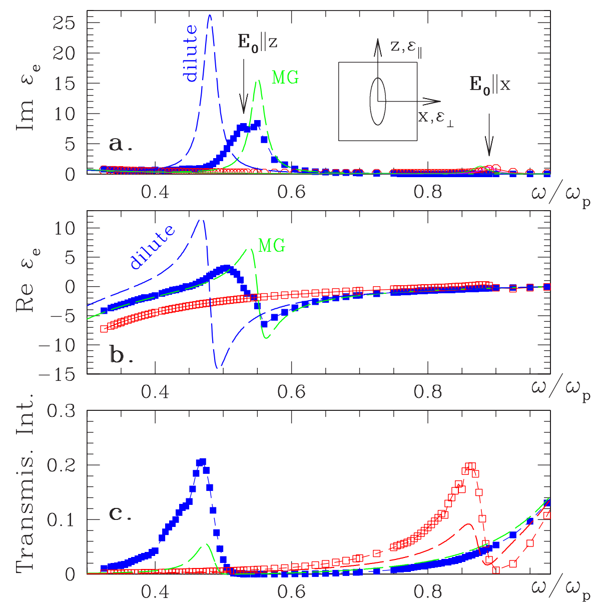

FIG. 3. (Color online) Transmission spectrum through an elliptical nanohole array for the p- and s-linear light polarizations. The p polarization is parallel to the [0,1] direction, while s is parallel to the [1,0] direction. (a) Im $\varepsilon_{xx}^{(e)}$ ($\mathbf{E_0}\|x$, p polarization) and Im $\varepsilon_{zz}^{(e)}$ ($\mathbf{E_0}\|z$, s polarization) vs ω/ω_p. (b) Re $\varepsilon_{xx}^{(e)}$ and Re $\varepsilon_{zz}^{(e)}$ vs ω/ω_p. In both polarizations there is a SP resonance peak at $\omega=\omega_{spx}$ and $\omega=\omega_{spz}$ (shown by the arrow), respectively. When $\mathbf{E_0}\|z$, the resonance shifts for larger values ($\omega_{spz}>\omega_{spx}$) and its amplitude reduces drastically. (c) Transmission coefficient T vs frequency ω, for different polarizations $\mathbf{E}\|x$ and $\mathbf{E}\|z$. The analytical results obtained using dilute and MG approximations are indicated by the dashed curves. The (connected by lines) filled and open symbols denote the results obtained numerically (Ref. 23) for a square array of holes in the shape of elliptical cylinders. Inset to (a): a unit cell with the elliptic hole and coordinate axes. The following sizes of the semiaxes were used: $a=0.1d$, $c=0.3d$, where d is the size of the unit cell. The film thickness is $h=100$ nm.

B. Rectangular holes

The depolarization factor n cannot be derived in the closed forms. That is, the resonance frequencies and the simple analytical expressions, such as Eqs. (11) and (12),

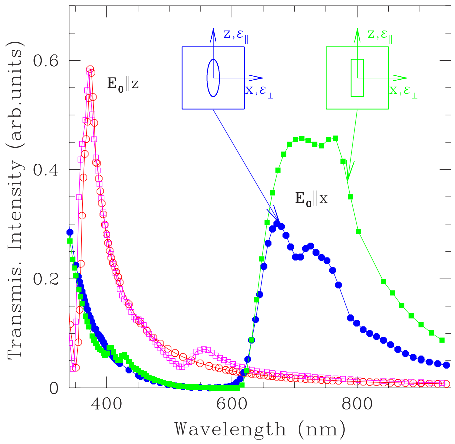

FIG. 4. (Color online) The similar to Fig. 3(c) drawings, but vs wavelength λ. The peak at λ ∼ 600–700 nm corresponds to $E_0\|x$ (i.e., p) polarization (shown in Fig. 2 of Ref. 5), while the peak at λ ∼ 400 nm corresponds to $E_0\|x$ polarization (not shown in Fig. 2 of Ref. 5). Filled and open circles show results obtained for the case of elliptical holes (see left-hand inset), while filled and open squares show results obtained for the case of rectangular holes (see right-hand inset). Insets: cross sections of the unit cell with the elliptical hole (left-hand side) and with the rectangular hole (right-hand side) used in our calculations. The elliptical hole's semiaxes are $a=0.1d$ and $c=0.3d$. The rectangular hole's sites are $l_x=2\times 0.1d$, $l_z=2\times 0.3d$, so that the aspect ratio of both geometries is the same $a/c=l_x/l_z=0.33$. d is the size of the unit cell. The film thickness is $h=100$ nm. $\omega_p=3\cdot 10^{15}$ rad/s.

cannot be obtained in the framework of the theory presented above for the rectangular holes. However, our numerical procedure provides us with a way to calculate the light transmission even in this case. The Fourier coefficient $\theta_{\mathbf{g}}$ of the $\theta(\mathbf{r})$ function [see Eq. (18)] for the rectangular inclusion is given by the following expression:[23]

$$\theta_{\mathbf{g}} = \left(\frac{2}{d}\right)^3 \left[\frac{\sin \frac{g_x l_x}{2}}{g_x}\right]\left[\frac{\sin \frac{g_y l_y}{2}}{g_y}\right]\left[\frac{\sin \frac{g_z l_z}{2}}{g_z}\right], \qquad (19)$$

where l_x, l_y, l_z are the sizes of the rectangular prism.

In Fig. 4 we show the light transmission $T(\omega)$ vs ω dependencies obtained numerically for light transmission through an array of rectangular holes with the same aspect ratio (minor site to major site) $l_x/l_z=0.33$. Since the cross section of the rectangular hole ($p=2a\times 2c=0.12$) is larger than that of the elliptic one ($\pi ac=0.094$), the peak of the light transmission [which is proportional to p, see Eq. (11)] at λ ∼ 700 nm is higher. The light transmission peaks at λ ∼ 400 nm for both rectangular and elliptical holes practically coincide. These results can be compared with results of Refs. 7, 9, and 12–15. Note that we have considered the metal parameter as well as the hole sizes to be consistent with Ref. 5. The sizes of the holes as well as the materials from which the perforated films were prepared, can be different in Refs. 7, 9, and 12–15 in comparison with Ref. 5 and our calculations, and, therefore, the resonance frequencies can also be different.

IV. SUMMARY AND DISCUSSION

Our method of calculation assumes that the holes size and the lattice constant of the hole lattice are small compared to the wavelength of light. We emphasize that in our calculations we have not used any absolute values (except for the film thickness, $h=100$ nm), but only relative ones—namely, the ratio between the holes sizes and the distance between the holes. In order to estimate the holes size in possible future experiments, for which our calculations are valid, we note that the expression for the cutoff frequency (i.e., the frequency in which the effective permittivity ε_e becomes negative) can be obtained from Eq. (11), $\omega_{\text{cutoff},i}=\sqrt{1-p}\,\omega_{sp,i}$. For p polarization (i.e., $\mathbf{E}_0\|x$) and the geometry used in Ref. 5, $\omega_{\text{cutoff}}\sim 0.5\omega_p$ (see Fig. 3), which for Au film corresponds to $\lambda_{\text{cutoff}}=2\pi c/\omega_{\text{cutoff}}\sim 600$ nm. As it can be seen from Fig. 4, the transmission peak for p polarization is pronounced in the range λ ∼ 600–900 nm. Therefore, the characteristic sizes of the holes should be smaller than 600 nm. Note that in the experiment described in Ref. 5, the hole sizes[32] were of the order ∼100–300 nm while the interhole distances were of the order ∼700 nm.

Even though we have used the quasistatic approximation, we believe that the effects predicted here for such holes sizes and lattice constants should persist even for lattice constants comparable with wavelength, as happens in most experiments to date. One reason for our belief is that, even though the spacing and wavelength are comparable, the electric field of a normally incident plane wave is uniform in the direction transverse to the wave propagation. The extension of the present calculations to this regime will be challenging, since the computation of transmission through a perforated metallic film is quite intricate when the wavelength and lattice constant are comparable. It would be of great interest if the present calculations could be extended into this regime.

In summary, we have studied analytically and numerically the extraordinary transmission through perforated metal films with elliptical holes. We have explained analytically the optical features found experimentally and described in Ref. 5. Our numerical results are in good agreement with experimental data. We also propose to use the magnetic field for getting a strong polarization effect, which depends on the ratio ω_c/ω_p. As a material which may be suitable for this purpose the bismuth can be considered, where the low carrier density ($\sim 3\times 10^{17}$ cm^{-1}) can make the carrier cyclotron energies, ω_c, equal to or greater than the plasmon energy, ω_p.[33] Another possibility is to use semiconducting materials like GaAs and InAs.[17,18,22,34]

ACKNOWLEDGMENTS

The author thankfully acknowledges useful conversations with David J. Bergman, Shlomo Havlin, Reuven Gordon, Yurii Kaganovskii, and Nilly Madar. This research was supported in part by grants from the Israel Science Foundation, and the KAMEA program of the Ministry of Absorption of the State of Israel.

*strelnik@mail.biu.ac.il

[1] T. W. Ebbesen, H. J. Lezec, H. F. Ghaemi, T. Thio, and P. A. Wolff, Nature (London) **391**, 667 (1998).

[2] H. Raether, *Surface Plasmons* (Springer-Verlag, Berlin, 1988).

[3] H. F. Ghaemi, T. Thio, D. E. Grupp, T. W. Ebbesen, and H. J. Lezec, Phys. Rev. B **58**, 6779 (1998); J. A. Porto, F. J. Garcia-Vidal, and J. B. Pendry, Phys. Rev. Lett. **83**, 2845 (1999); L. Martin-Moreno, F. J. Garcia-Vidal, H. J. Lezec, K. M. Pellerin, T. Thio, J. B. Pendry, and T. W. Ebbesen, *ibid.* **86**, 1114 (2001); L. Yin, V. K. Vlasko-Vlasov, A. Rydh, J. Pearson, U. Welp, S.-H. Chang, S. K. Gray, G. C. Schatz, D. B. Brown, and C. W. Kimball, Appl. Phys. Lett. **85**, 467 (2004); C. Genet and T. W. Ebbesen, Nature (London) **445**, 39 (2007), and references therein.

[4] E. Popov, M. Neviere, S. Enoch, and R. Reinisch, Phys. Rev. B **62**, 16100 (2000).

[5] R. Gordon, A. G. Brolo, A. McKinnon, A. Rajora, B. Leathem, and K. L. Kavanagh, Phys. Rev. Lett. **92**, 037401 (2004).

[6] M. Sarrazin and J.-P. Vigneron, Opt. Commun. **240**, 89 (2004).

[7] K. J. Klein Koerkamp, S. Enoch, F. B. Segerink, N. F. van Hulst, and L. Kuipers, Phys. Rev. Lett. **92**, 183901 (2004).

[8] H. Cao and A. Nahata, Opt. Express **12**, 3664 (2004).

[9] A. Degiron, H. J. Lezec, N. Yamamoto, and T. W. Ebbesen, Opt. Commun. **239**, 61 (2004).

[10] J. Elliott, I. I. Smolyaninov, N. I. Zheludev, and A. V. Zayats, Opt. Lett. **29**, 1414 (2004).

[11] M. Mansuripur, A. R. Zakharian, and J. V. Moloney, Opt. Photonics News **15**, 36 (2004).

[12] K. L. van der Molen, K. J. Klein Koerkamp, S. Enoch, F. B. Segerink, N. F. van Hulst, and L. Kuipers, Phys. Rev. B **72**, 045421 (2005).

[13] F. J. Garcia-Vidal, E. Moreno, J. A. Porto, and L. Martin-Moreno, Phys. Rev. Lett. **95**, 103901 (2005); F. J. Garcia-Vidal, L. Martin-Moreno, E. Moreno, L. K. S. Kumar, and R. Gordon, Phys. Rev. B **74**, 153411 (2006).

[14] A. Degiron and T. W. Ebbesen, J. Opt. A, Pure Appl. Opt. **7**, S90 (2005).

[15] M.-W. Tsai, T.-H. Chuang, H.-Y. Chang, and D.-C. Lee, Appl. Phys. Lett. **89**, 093102 (2006).

[16] J. H. Kim and P. J. Moyer, Appl. Phys. Lett. **89**, 121106 (2006).

[17] Y. M. Strelniker and D. J. Bergman, Phys. Rev. B **59**, R12763 (1999).

[18] D. J. Bergman and Y. M. Strelniker, Phys. Rev. Lett. **80**, 857 (1998).

[19] Y. M. Strelniker and D. J. Bergman, Eur. Phys. J. A **7**, 19 (1999); D. J. Bergman and Y. M. Strelniker, Physica B **279**, 1 (2000).

[20] Y. M. Strelniker, D. Stroud, and A. O. Voznesenskaya, Eur. Phys. J. B **52**, 1 (2006); Y. M. Strelniker, D. Stroud, and A. O. Voznesenskaya, J. Appl. Phys. **99**, 08H702 (2006).

[21] A. Garcia-Martin, G. Armelles, and S. Pereira, Phys. Rev. B **71**, 205116 (2005); L. E. Helseth, *ibid.* **72**, 033409 (2005); V. I. Belotelov, L. L. Doskolovich, and A. K. Zvezdin, Phys. Rev. Lett. **98**, 077401 (2007); R. H. Tarkhanyan, and D. G. Niarchos, Opt. Express **14**, 5433 (2006); D. M. Newman, M. L. Wears, and R. J. Matelon, Europhys. Lett. **68**, 692 (2004); G. Duchs, G. L. J. A. Rikken, T. Grenet, and P. Wyder, Phys. Rev. Lett. **87**, 127202 (2001).

[22] I. V. Kukushkin, J. H. Smet, S. A. Mikhailov, D. V. Kulakovskii, K. von Klitzing, and W. Wegscheider, Phys. Rev. Lett. **90**, 156801 (2003).

[23] Y. M. Strelniker and D. J. Bergman, Phys. Rev. B **50**, 14001 (1994); D. J. Bergman and Y. M. Strelniker, *ibid.* **49**, 16256 (1994).

[24] D. J. Bergman and D. Stroud, Solid State Phys. **45**, 147 (1992).

[25] G. W. Milton, *The Theory of Composites* (Cambridge University Press, Cambridge, 2002).

[26] D. J. Bergman and Y. M. Strelniker, Phys. Rev. B **60**, 13016 (1999).

[27] D. J. Bergman and Y. M. Strelniker, Phys. Rev. B **59**, 2180 (1999).

[28] L. D. Landau, E. M. Lifshitz, and L. P. Pitaevskii, *Electrodynamics of Continuous Media* (Pergamon, Oxford, 1984).

[29] G. Hass and L. Hadley, “Optical properties of metals,” in American Institute of Physics Handbook, 3rd ed., edited by D. E. Gray (AIP, New York, 1972), pp. 6–133.

[30] A. M. Dykhne, A. K. Sarychev, and V. M. Shalaev, Phys. Rev. B **67**, 195402 (2003).

[31] J. R. DiMaio and J. Ballato, Opt. Express **14**, 2380 (2006).

[32] R. Gordon, M. Hughes, B. Leathem, K. L. Kavanagh, and A. G. Brolo, Nano Lett. **5**, 1243 (2005).

[33] R. E. Sherriff and R. P. Devaty, Phys. Rev. B **41**, 1340 (1990); **48**, 1525 (1993); L. M. Claessen, A. G. M. Jansen, and P. Wyder, *ibid.* **33**, 7947 (1986); G. J. Strijkers, F. Y. Yang, D. H. Reich, C. L. Chien, P. C. Searson, Y. M. Strelniker, and D. J. Bergman, IEEE Trans. Magn. **37**, 2067 (2001).

[34] M. Tornow, D. Weiss, K. v. Klitzing, K. Eberl, D. J. Bergman, and Y. M. Strelniker, Phys. Rev. Lett. **77**, 147 (1996).